forests

MDPI

Article

Spatiotemporal Variation in Vegetation and Its Driving Mechanisms in the Southwest Alpine Canyon Area of China

Jinlin Lai [1], Tianheng Zhao [1] and Shi Qi [1,2,*]

[1] School of Soil and Water Conservation, Beijing Forestry University, Beijing 100083, China; jinlin@bjfu.edu.cn (J.L.); zhaotianheng@bjfu.edu.cn (T.Z.)
[2] Key Laboratory of Soil and Water Conservation State Forestry Bureau, Beijing 100083, China
* Correspondence: qishi@bjfu.edu.cn

Abstract: The Southwest Alpine Canyon Area (SACA), a well-known ecological vulnerability region, plays a very important role in China. Identifying the driving force of the spatial heterogeneity of vegetation and the response of interannual vegetation changes to climate change and human activities would be helpful for ecosystem management. Based on the NDVI dataset, the study analyzed the trend of NDVI change from 2000 to 2019 using the Theil–Sen trend analysis and the Mann–Kendal significance test, detected the driving forces of the spatial heterogeneity of NDVI by the means of the geographical detector, and analyzed the relative contribution of climate change and human activities to interannual NDVI changes using residual analysis model. The results showed that, in terms of the spatial distribution, the pattern of NDVI showed that it is higher in the southeast and lower in the northwest region of the SACA. Elevation was the dominant factor influencing the spatial heterogeneity of NDVI, with the explanatory power of 64%, much larger than other factors, and vegetation type, temperature, precipitation, land use type, and soil type were the main factors. In addition, the explanatory power of the dual factor interaction was higher than that of the single factor effect, which showed two kinds of interaction relationships: bivariate enhancement and nonlinear enhancement. In terms of the temporal variation, 85.59% of the study area showed an increasing trend, and only 14.41% of the area showed a decreasing trend. The main factor affecting NDVI changes was human activities, and climate change was the secondary factor, with relative contributions of 71.35% and 28.65%, respectively. The study will promote a better understanding of the complex mechanisms of vegetation changes and provide scientific recommendations for the prevention of vegetation degradation and vegetation restoration in the SACA.

Keywords: vegetation change; remote sensing; normalized difference vegetation index; climate change; human activities; geographical detector; residual analysis

Citation: Lai, J.; Zhao, T.; Qi, S. Spatiotemporal Variation in Vegetation and Its Driving Mechanisms in the Southwest Alpine Canyon Area of China. *Forests* **2023**, *14*, 2357. https://doi.org/10.3390/f14122357

Academic Editor: Nikolay Strigul

Received: 1 November 2023
Revised: 21 November 2023
Accepted: 27 November 2023
Published: 30 November 2023

1. Introduction

Terrestrial vegetation is an important component of ecosystems and plays an indispensable role in ecosystem carbon balance, climate regulation, and water conservation [1–3]. However, the vegetation variation due to rapid climate change and intensified human activities has led to imbalances in terrestrial ecosystems indirectly and to many other ecological and environmental problems [4]. Especially in the high latitude and altitude zones, including the SACA, compared with other regions, the speed of temperature rise is significantly faster and the precipitation in the SACA has generally shown a decreasing trend since 2000. The regional climate has been represented as "warming and drying", and the frequency of extreme heat events has increased significantly, affecting the vegetation growth [5]. The impacts of human activities on vegetation changes have been paid more attention, including urbanization, agricultural expansion, and ecological restoration projects, which directly or indirectly affect the ecosystem balance and health [6,7]. Therefore, the study of vegetation response to climate change and human activities has become a popular

topic, which is essential to understand the spatiotemporal characteristics of vegetation and its response mechanisms to environmental factors, and also helps in decision-making for vegetation management and sustainable development.

Climatic conditions are the bases for vegetation growth, and their changes further influence plant photosynthesis, soil respiration, and organic carbon decomposition [8]. Over a longer period, it can even change the potential vegetation types of a region [9]. Temperature and precipitation have been considered to be the main climatic factors affecting vegetation growth [10,11]. Temperature variation directly affects vegetation phenology, physiological metabolism, and distribution patterns [12]. As the temperature rises, vegetation phenology tends to shift to an earlier date, leading to the enhancement of plant photosynthesis and water utilization efficiency, thus stimulating vegetation growth [13,14]. However, when the temperature rises to over a certain threshold, plant photosynthesis is inhibited, while respiration is enhanced, nutrient consumption increases, and vegetation growth is inhibited [15,16]. The effect of precipitation on vegetation is more obvious in arid and semi-arid regions, where the vegetation is more sensitive to precipitation variation due to the effect of water deficit, and the increase in precipitation can effectively enhance the available soil water content to promote the activity of root system [17]. In humid areas, excessive precipitation can lead to a deficit of oxygen supply in the soil, affecting breath and nutrient absorption of root system and resulting in restricted vegetation growth [18,19]. However, solar radiation is often overlooked in research. Solar radiation, the source of energy for plant photosynthesis, can enhance the efficiency of plant photosynthesis when an appropriate amount of solar radiation is received, thus promoting vegetation growth, and on the contrary, excessive solar radiation can increase the plant evapotranspiration and inhibit the vegetation photosynthesis, leading to a slowdown of plant metabolism and growth [20,21].

Studies have shown that about 30% to 50% of the global land cover has been affected by human activities, and there are obvious differences in the degree of human activities' impacts on different land cover types [22]. Therefore, in previous studies, land cover change has often been used as an important means for examining the impact of human activities on vegetation change, which varies corresponding to different land cover scenarios [23]. The impact of human activities on vegetation growth represents duality, and on the one hand, land use changes such as accelerating urbanization, the rapid expansion of construction sites, overgrazing, deforestation, and poorly planned agricultural reclamation caused by human activities are the main causes of vegetation degradation and destroy natural vegetation [24]; on the other hand, the implementation of forestry ecological engineering projects in China have made vegetation changes to increase land cover [25], in which land use changes induced by afforestation are the main cause of vegetation improvement in China. In the past 20 years, a series of forestry ecological engineering projects, including returning farmland to forests and grasslands project, the natural forest resources protection project, and comprehensive treatment project of karst rocky desertification have been implemented in China, which significantly increase the vegetation coverage and obviously improve the ecological environment [26].

The SACA, located in the Qinghai–Tibet Plateau with a unique topography and apparently a unique spatial heterogeneity, is an ecologically vulnerable zone where the ecosystem is very sensitive and unstable to climate change. In recent years, some scholars have analyzed the spatiotemporal vegetation evolution at different spatiotemporal scales and its driving forces using different methods such as trend analysis, correlation analysis, statistics, and geographic spatial analysis techniques [27,28]. In terms of the spatial distribution, the vegetation cover in the SACA showed a spatial distribution pattern of "high in the southeast and low in the northwest", and the spatial distribution characteristics of temperature and precipitation were similar to those of the vegetation cover, and they explained well the variability in the spatial distribution of the regional vegetation [29]. In terms of temporal changes, the overall vegetation cover in the SACA has increased significantly in the last 20 years, which is significantly correlated with temperature and precipitation changes,

where the vegetation cover shows a positive correlation with temperature changes and a negative correlation with precipitation changes [30]. In addition, among the anthropogenic factors, the implementation of forestry ecological projects effectively restored the regional vegetation, which was the main reason for the improvement of vegetation cover [31]. The secondary reason is the influence of urbanization, and the recent study on the characteristics of vegetation dynamics under county-scale urbanization found that the impacts of urbanization on vegetation change showed a significant spatial heterogeneity due to the differences in natural background and economic development stages and represented a "U"-shaped relationship between urbanization rate and the slope of NDVI change [32]. Although some analyses have been conducted on the impacts of climate change and human activities on the vegetation change in the SACA, there is still a lack of systematic research on the driving mechanism of this vegetation change. When analyzing the influence of climate factors on vegetation change, only temperature and precipitation were considered, while solar radiation was ignored, and its influence on vegetation change needs to be clarified. The effect of land use type changes on vegetation should be considered. Previous studies on vegetation change and influencing factors in the SACA mostly focused on a specific type, or a few indicators, without explicitly clearing the climate change and the impacts of human activities, and the spatial interactions between them.

The objectives of this study are as follows: (1) to reveal the spatiotemporal characteristics of NDVI in the SACA during the past 20 years; (2) to detect the driving forces of NDVI spatial heterogeneity; and (3) to assess the relative roles of climate change and human activities on the changes in NDVI. It may provide a scientific basis for the monitoring, management, and protection of vegetation dynamics in the SACA; furthermore, sustainable forest management interventions can be proposed in a more targeted manner for achieving the goal of green and sustainable development.

2. Study Area

The SACA is located at the junction of Sichuan, Tibet, and Yunnan provinces, with an area of about 61.10×10^4 km^2 and geographical coordinates between 24°58′7.47″~32°51′24.93″ N and 91°23′48.24″~104°13′43.55″ E. The elevation ranges from 88 to 6830 m, the terrain is undulating and complex, and the landscape is dominated by mountains, hills, and plateaus (Figure 1). The climate changes from the southeast to the northwest across arid, semi-arid, semi-humid, and humid zones, with an average temperature of −2.98~21.89 °C and an average precipitation of 296.62~2302.90 mm. According to the soil and water conservation function zoning, it can be divided into Northwest Yunnan Alpine Canyon Ecological Maintenance Area (NYAC), North Yunnan–Southwest Sichuan Alpine Canyon Water Storage and Soil Conservation Area (NYSS), East Tibet–West Sichuan Alpine Canyon Ecological Maintenance Water Containment Area (ETWS), and Southeast Tibet Alpine Canyon Ecological Maintenance Area (STAC) (Figure 1).

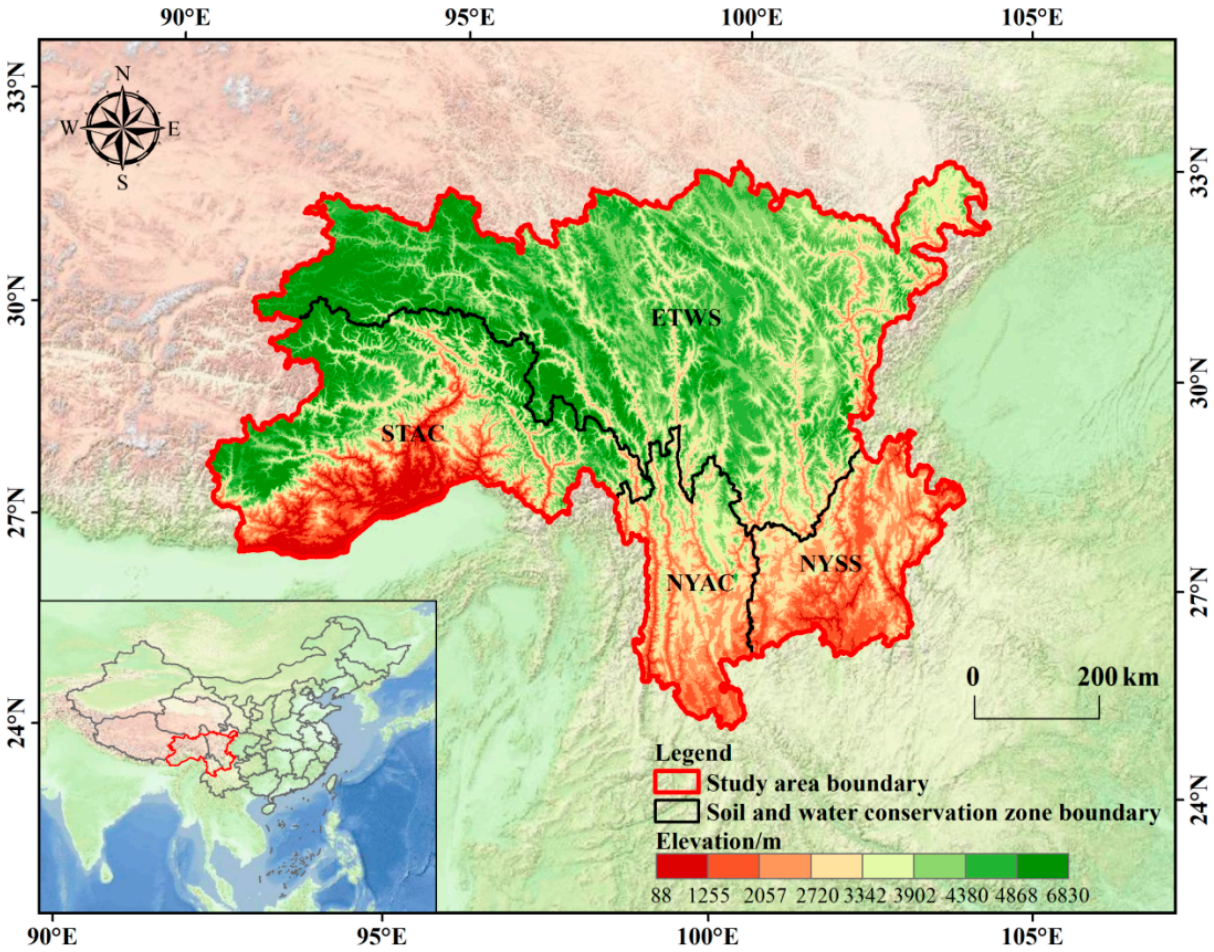

Figure 1. Geographic location of the study area.

3. Data and Methods

3.1. Data Sources and Processing

The NDVI data were obtained from the SPOT vegetation NDVI dataset of the Resource and Environmental Science and Data Center of the Chinese Academy of Sciences (https://www.resdc.cn/, accessed on 10 September 2023), spanning from January 2000 to December 2019, with a spatial resolution of 1 km, and the maximum value synthesis method was used to calculate the annual NDVI dataset (Table 1). Climatic factor data mainly include temperature, precipitation, and solar radiation datasets, of which the temperature and precipitation datasets were obtained from the National Earth System Science Data Center (http://www.geodata.cn, accessed on 12 September 2023), and the solar radiation dataset was obtained from worldclim (https://worldclim.org/, accessed on 12 September 2023), whose spatial resolutions were all 1 km. The dataset was cropped using the ArcGIS (Version 10.2 (2013), Environmental Systems Research Institute, Redlands, CA, USA, https://www.esri.com, accessed on 10 September 2023) to obtain the dataset of climate factors in the SACA. The DEM was downloaded from Geospatial Data Cloud (https://www.gscloud.cn/, accessed on 12 September 2023) with a spatial resolution of 30 m, and its spatial resolution was changed to 1 km using resampling. After this, the DEM of the study area was obtained by cropping, and the slope was further extracted. Vegetation type, soil type, land use type, population density, and GDP data were obtained from the Environmental Science and Data Center of the Chinese Academy of Sciences with a spatial resolution of 1 km, and the above datasets were obtained by cropping.

Table 1. Data sources in this study.

Categories	Factors	Abbreviations	Spatial Resolution	Source
NDVI			1 km	Resource and Environmental Sciences Data Center (https://www.resdc.cn/)
Natural factors	Elevation	Ele	30 m	Geospatial Data Cloud (https://www.gscloud.cn/sources/, accessed on 12 September 2023)
	Slope	Slo	30 m	
	Solar radiation	Sol	1 km	National Earth System Science
	Precipitation	Pre	1 km	Data Center (http://www.geodata.cn/,
	Temperature	Tem	1 km	accessed on 12 September 2023)
	Soil type	Soi	1 km	Resource and Environmental Sciences Data Center
	Vegetation type	Veg	1 km	(https://www.resdc.cn/, accessed on 12 September 2023)
Anthropogenic factors	Land use type	Lut	1 km	Resource and Environmental Sciences Data Center (https://www.resdc.cn/, accessed on 12 September 2023)
	GDP	GDP	1 km	
	Population density	Pop	1 km	

3.2. Methods

3.2.1. The Trends Analysis

The Theil–Sen trend analysis [33] was used to calculate the change slope (θ) of time series data. Then, the Mann–Kendall (MK) significance test [34] was used to determine whether the change trends were significant. Based on the change slope (θ) and significance level (p-value), the NDVI trend was classified into four types: significant decrease ($\theta < 0$, $p < 0.05$), insignificant decrease ($\theta < 0$, $p \geq 0.05$), insignificant increase ($\theta > 0$, $p \geq 0.05$), and significant increase ($\theta > 0$, $p < 0.05$).

3.2.2. Correlation Analysis

The study examined the impact of climate factors on vegetation growth by analyzing pixel-by-pixel correlations and significance using partial correlation coefficients and t-tests to reveal how NDVI responds to specific climate changes [35–37]. According to the partial correlation coefficient (R) and significance level (p-value), the degree of correlation was classified into four types: significant negative correlation ($R < 0$, $p < 0.05$), insignificant negative correlation ($R < 0$, $p \geq 0.05$), insignificant positive correlation ($R > 0$, $p \geq 0.05$), and significant positive correlation ($R > 0$, $p < 0.05$).

3.2.3. Geographical Detector Model

The geographical detector was employed to assess the driving forces of the influence factors on the spatial heterogeneity of NDVI. In this study, the geographical detector was used to measure the magnitude of their influence, represented by the q value ($0 \leq q \leq 1$), where a higher q value indicates a stronger influence. The formula for calculating the q value is as follows [38,39]:

$$q = 1 - \frac{\mathrm{SSW}}{\mathrm{SST}} \quad (1)$$

$$\mathrm{SSW} = \sum_{h=1}^{L} N_h \rho_h^2 \quad (2)$$

$$\mathrm{SST} = N\rho^2 \quad (3)$$

where $h = 1, 2, 3 \ldots L$ is the stratification of the independent variable X; N_h is the number of units in stratum h; N is the number of units in the whole region; ρ_h^2 is the variance of the h layer; and ρ^2 is the variance of the whole region. SST represents the within-layer variance; SSW represents the sum of variance of the whole region.

The function of the interaction detector is to identify the interactive effects between different factors. First, the q values of the independent variables X_1 and X_2 are denoted as $q(X_1)$ and $q(X_2)$, and then, $q(X_1 \cap X_2)$ is calculated for the interaction of the independent variables X_1 and X_2, and $q(X_1 \cap X_2)$ is compared with the values of $q(X_1)$ and $q(X_2)$ to determine whether the interactive effects of the independent variables X_1 and X_2 have an

enhanced or weakened influence on the dependent variable Y. The specific judgment basis is shown in Table 2.

Table 2. The types of interactions and judgment bases.

Judgment Basis	Role Relationship
$q(X_1 \cap X_2) < \text{Min}\,[q(X_1), q(X_2)]$	Nonlinear weakening
$\text{Min}\,[q(X_1), q(X_2)] < q(X_1 \cap X_2) < \text{Max}\,[q(X_1), q(X_2)]$	Single-factor nonlinear attenuation
$q(X_1 \cap X_2) > \text{Max}\,[q(X_1), q(X_2)]$	Bivariate enhancement
$q(X_1 \cap X_2) = q(X_1) + q(X_2)$	Independent
$q(X_1 \cap X_2) > q(X_1) + q(X_2)$	Nonlinear enhancement

3.2.4. Residual Analysis Model and Calculation of Relative Contribution

The residual analysis can quantitatively separate the effects of climate change and human activities on vegetation [40]. By constructing a multiple regression analysis model between NDVI and climate factors, the predicted value ($NDVI_{CC}$) was obtained to characterize the effect of climate change on NDVI, while the difference ($NDVI_{HA}$) between the NDVI value extracted from remote sensing images and $NDVI_{CC}$ characterizes the effect of HA on NDVI. The mathematical expression of the model is as follows:

$$NDVI_{HA} = NDVI - NDVI_{CC} \quad (4)$$

$$NDVI_{CC} = a \times P(i,t) + b \times T(i,t) + c \times S(i,t) + d \quad (5)$$

where a, b, c, and d represent regression coefficients; P is the annual precipitation; T is the average annual temperature; and S is the annual solar radiation.

The drivers of NDVI changes were categorized based on $NDVI_{HA}$, $NDVI_{CC}$, and NDVI change slope, and their relative contributions were quantified using specific classification criteria and a formula for calculation [41,42], as detailed in Table 3.

Table 3. Identification of drivers of NDVI change and calculation of relative contribution.

θ			Drivers	Relative Contribution of Climate Change	Relative Contribution of Human Activities
NDVI	$NDVI_{HA}$	$NDVI_{CC}$			
>0	>0	>0	CC&HA	$\frac{\lvert\theta(NDVI_{CC})\rvert}{\lvert\theta(NDVI_{CC})\rvert+\lvert\theta(NDVI_{HA})\rvert}$	$\frac{\lvert\theta(NDVI_{HA})\rvert}{\lvert\theta(NDVI_{CC})\rvert+\lvert\theta(NDVI_{HA})\rvert}$
	>0	<0	HA	100%	0
	<0	>0	CC	0	100%
<0	<0	<0	CC&HA	$\frac{\lvert\theta(NDVI_{CC})\rvert}{\lvert\theta(NDVI_{CC})\rvert+\lvert\theta(NDVI_{HA})\rvert}$	$\frac{\lvert\theta(NDVI_{HA})\rvert}{\lvert\theta(NDVI_{CC})\rvert+\lvert\theta(NDVI_{HA})\rvert}$
	<0	>0	HA	100%	0
	>0	<0	CC	0	100%

Note: CC and HA represent climate change and human activities, respectively.

4. Results and Analysis

4.1. Characteristics of Spatiotemporal Variations in NDVI

4.1.1. Spatial Distribution Pattern in NDVI

The SACA exhibits a high level of vegetation cover, with mean NDVI values of 0.60, 0.64, and 0.69 in 2000, 2010, and 2019, respectively. Significant spatial variations in NDVI distribution are observed, and the areas with medium-high and high vegetation cover are primarily concentrated in the NYAC, NYSS, Southern STAC, and Eastern ETWS. The areas with low and medium-low vegetation cover are primarily situated in the northwestern part of the study area (Figure 2). From 2000 to 2019, the proportion of the areas with high vegetation cover increased from 7.78% to 43.82%, which was mainly transformed by the areas with medium-high vegetation cover, resulting in a reduction in the percentage of the areas with medium-high vegetation cover, particularly in the NYAC and NYSS. The

proportion of areas with medium vegetation cover showed a decreasing trend, transforming into areas with medium-high vegetation cover, mainly located in the Eastern ETWS. The proportion of the areas with low and medium-low vegetation cover remained relatively stable, hovering around 13%.

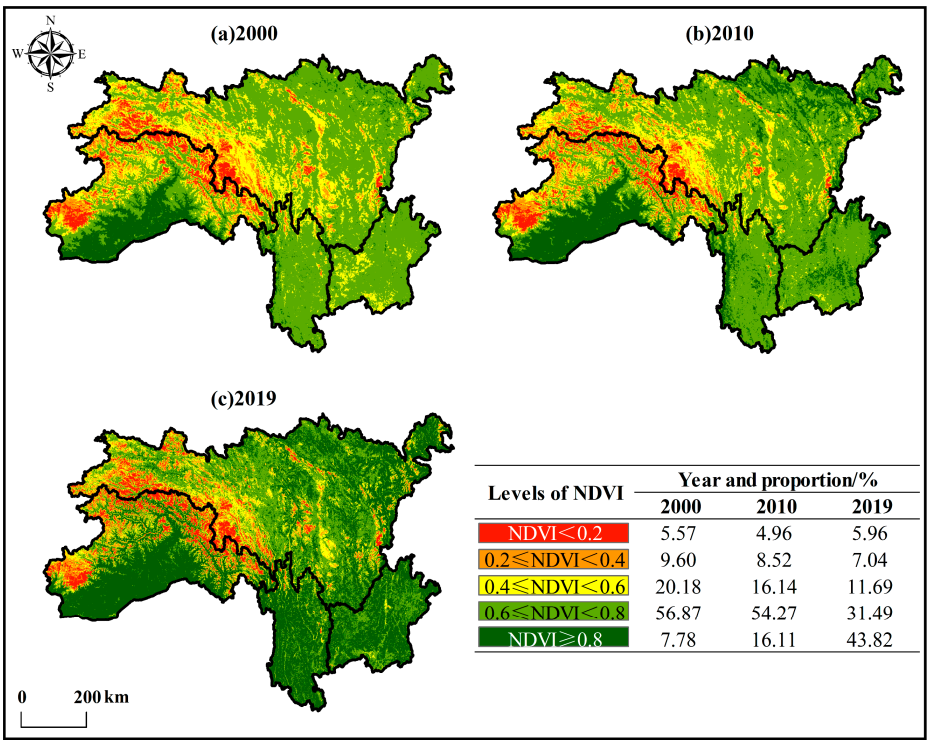

Levels of NDVI	Year and proportion/%		
	2000	2010	2019
NDVI < 0.2	5.57	4.96	5.96
0.2 ≤ NDVI < 0.4	9.60	8.52	7.04
0.4 ≤ NDVI < 0.6	20.18	16.14	11.69
0.6 ≤ NDVI < 0.8	56.87	54.27	31.49
NDVI ≥ 0.8	7.78	16.11	43.82

Figure 2. Spatial distribution of NDVI in (**a**) 2000, (**b**) 2010, and (**c**) 2019. Note: low vegetation cover (NDVI < 0.2), medium-low vegetation cover (0.2 ≤ NDVI < 0.4), medium vegetation cover (0.4 ≤ NDVI < 0.6), medium-high vegetation cover (0.6 ≤ NDVI < 0.8), and high vegetation cover (NDVI ≥ 0.8).

4.1.2. Temporal Variation Characteristics in NDVI

The NDVI in the SACA from 2000 to 2019 showed an increasing trend, with the mean value of the change slope (θ) of 0.0022 (Figure 3a), and the proportion of areas with $\theta > 0$ was 85.59%, of which the ones that achieved the required significance level ($p < 0.05$) accounted for 66.72%, and they were mainly distributed in the NYAC, NYSS, Northern ETWS, and Southern STAC. The percentage of the areas with a decreasing trend of NDVI was 14.41%, with 3.71% of the area achieving the required significance level ($p < 0.05$), mainly distributed at the junction of the ETWS and the STAC (Figure 3b).

4.2. Characteristics of Climate Change and the Correlation Analysis of NDVI Change

4.2.1. Spatiotemporal Variation Characteristics of Climate Factors

The study used the Theil–Sen trend method to analyze the characteristics of climate factor changes, and the results showed that the overall climate change in the SACA from 2000 to 2019 showed "warming and drying". The temperature in the region showed an increasing trend, with an increase ranging from 0.002 to 0.046 °C·a^{-1}, and a mean value of 0.02 °C·a^{-1}. The larger increase was observed in the STAC and the Western ETWS, while other regions exhibited smaller increases (Figure 4a). The precipitation exhibited a fluctuation range of −19.23 to 10.69 mm·a^{-1}, with a mean value of −3.97 mm·a^{-1}. Overall, 77.28% of the study area, with a decreasing trend, was located in the southwestern part of the study area. The proportion of areas with an increasing trend was 22.72%, primarily in the Eastern NYSS and the Northern ETWS (Figure 4b). The fluctuation range of solar radiation was −33.17 to 77.97 MJ·m^{-2}·a^{-1}, with a mean value of 6.92 MJ·m^{-2}·a^{-1}.

Approximately 25.73% of the study area displayed a decreasing trend, mainly in the STAC and the Northern ETWS, while the rest of the region (74.27%) showed an increasing trend (Figure 4c).

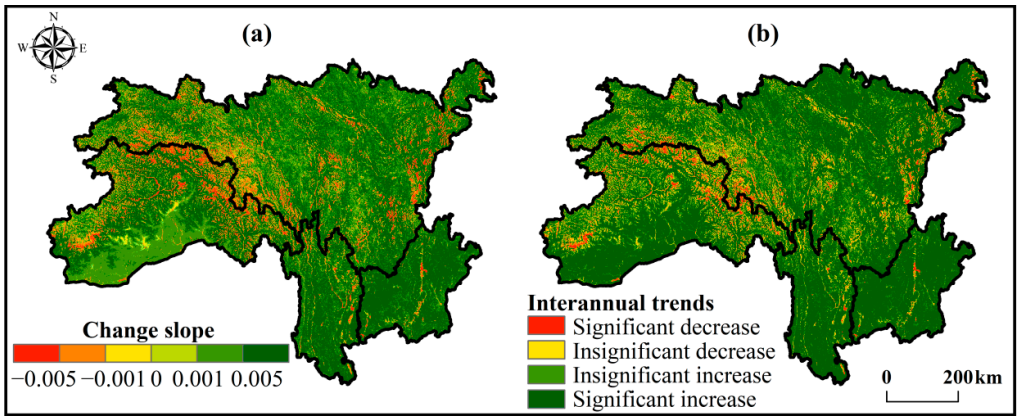

Figure 3. Spatial distribution of (**a**) change slope and (**b**) interannual trends.

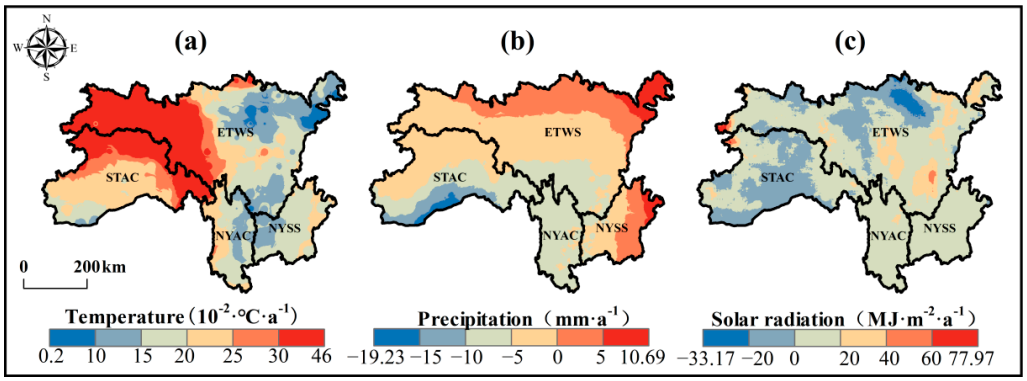

Figure 4. Spatial distribution of trends for climate factors: (**a**) temperature, (**b**) precipitation; (**c**) solar radiation.

4.2.2. Correlation Analysis between Climate Factors and NDVI

The study analyzed the correlation between NDVI and the time series changes in temperature, precipitation, and solar radiation from 2000 to 2019, utilizing partial correlation coefficients and *t*-tests. The results indicated that the proportion of areas with a positive correlation between NDVI and temperature was 78.02% (23.22%, $p < 0.05$), mainly distributed in the northern part of the study area. The proportion of negatively correlated areas was 21.98% (2.76%, $p < 0.05$), concentrated at the junction of the ETWS and the STAC (Figure 5a,b). For NDVI and precipitation, approximately 46.92% of the study area showed a positive correlation (7.98%, $p < 0.05$), concentrated in the Northern ETWS and the Eastern NYSS. Meanwhile, 53.08% of the study area exhibited a negative correlation (10.25%, $p < 0.05$), mainly in the southwestern region of the study area (Figure 5c,d). Concerning NDVI and solar radiation, around 64.62% of the study area displayed a positive correlation (11.18%, $p < 0.05$), mainly in the central and northeastern parts of the study area. The remaining 35.38% of the study area exhibited a negative correlation (4.04%, $p < 0.05$), primarily in the Northern ETWS (Figure 5e,f).

Overall, among the climatic factors, the highest percentage of partial correlation coefficients that passed the significance test was 25.98% for NDVI and temperature, indicating that temperature is the dominant climatic factor influencing NDVI changes. In the ETWS, the proportions of the areas where the partial correlation coefficients passed the significance test were the highest among all regions, with precipitation and NDVI, temperature and NDVI, and solar radiation and NDVI showing significant correlation proportions of 21.90%,

28.57%, and 17.94%, respectively. This suggests that the ETWS is more sensitive to climate change than other regions and is susceptible to its impacts.

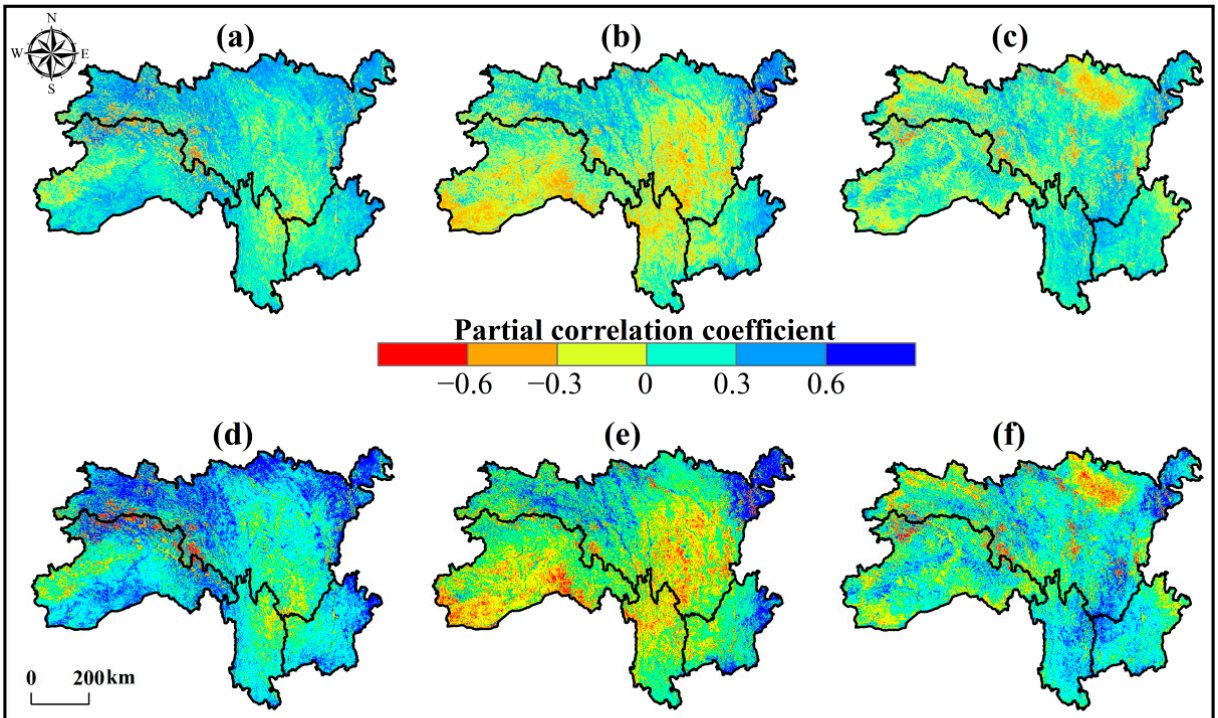

Climate factors	Levels of significance test and their proportion/%			
	Significant negative correlation	Insignificant negative correlation	Insignificant positive correlation	Significant positive correlation
Temperature	2.76	19.22	54.80	23.22
Precipitation	10.25	42.83	38.94	7.98
Solar radiation	4.04	31.34	53.44	11.18

Figure 5. Spatial distribution of partial correlation coefficients between NDVI and (**a**) temperature, (**c**) precipitation, and (**e**) solar radiation and their significance tests (**b**,**d**,**f**).

4.3. Analysis of Land Use Type Change

The transformation of land use type can visually reflect the alteration in natural land by HA, and this transformation significantly influences vegetation changes. According to the results of Figure 6 and Table 4, it can be seen that forest and grassland are the main land use type in the SACA, with each accounting for more than 38% of the study area in both 2000 and 2018. They are followed by bare land, occupying more than 9% of the study area, while the share of other land use types remains relatively small, with none exceeding 5%. The SACA experienced significant land use type transformations from 2000 to 2018, affecting an area of 231,851 km^2, which accounts for 37.94% of the study area. During this period, the areas covered by water and bare land decreased, totaling 5172 km^2 and 24,257 km^2, respectively. Other land use types increased in area, especially forest and grassland, which had the highest increase in area, which were 12,637 km^2 and 13,773 km^2, respectively. This increase was mainly due to the conversion of bare land into forest and grassland, aside from mutual transformations between the two. Construction land exhibited the highest growth rate among land use types, increasing from 507 km^2 in 2000 to 1172 km^2 in 2018 and representing a growth rate of 131.16%. This growth is a consequence of economic development and rapid urban expansion.

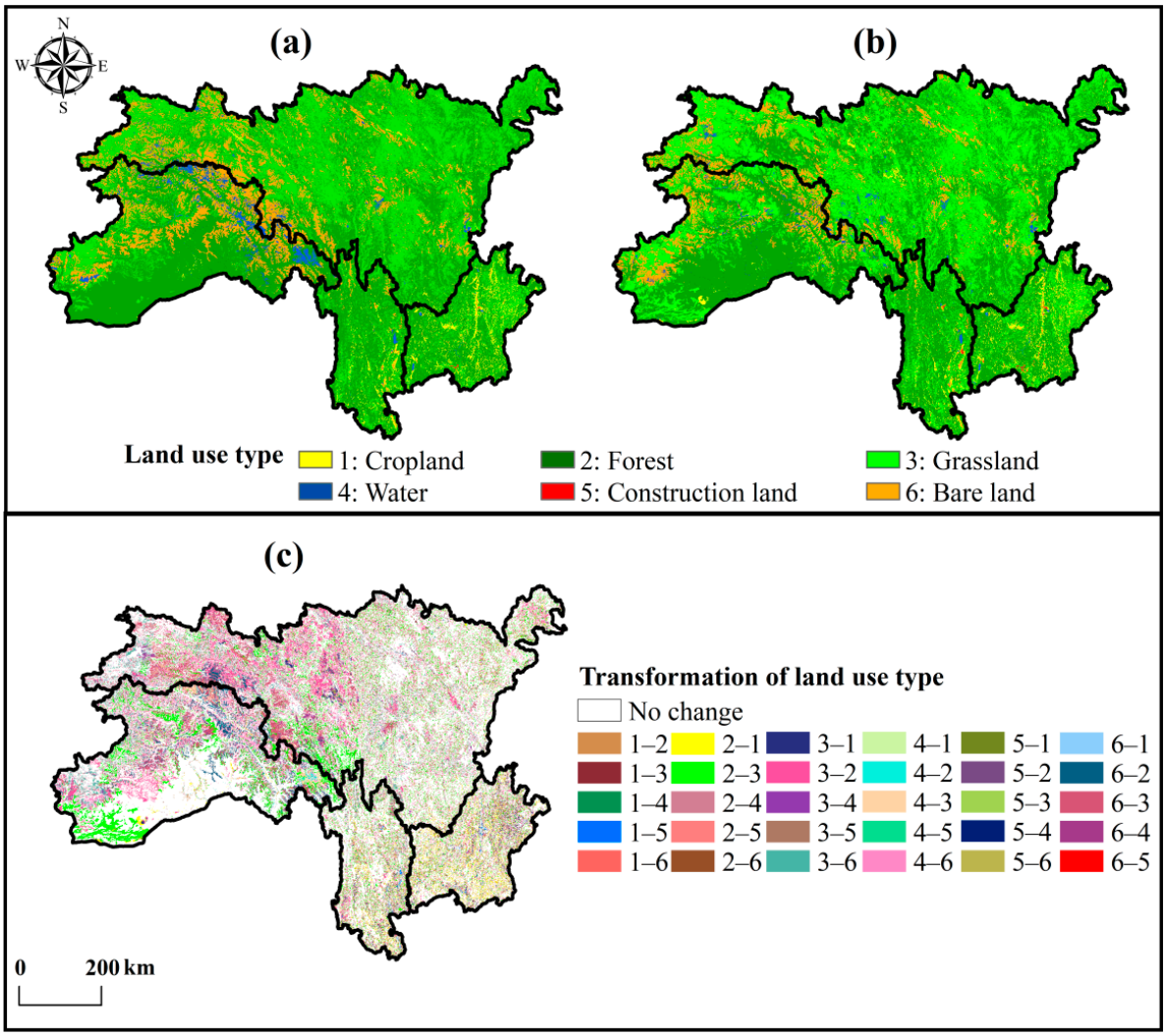

Figure 6. Spatial distribution of land use type in (**a**) 2000 and (**b**) 2018, and (**c**) their changes from 2000 to 2018.

Table 4. Transfer matrix of land use type change (area: km^2).

Land Use Type		2018						
		To Cropland	To Forest	To Grassland	To Water	To Construction Land	To Bare Land	Total
2000	From cropland	9074	7916	5325	381	459	42	23,197
	From forest land	8958	189,284	57,610	1436	158	3909	261,355
	From grassland	6923	61,944	146,471	1890	272	14,987	232,487
	From water	270	1655	4486	2939	19	4808	14,177
	From construction land	201	58	78	25	126	19	507
	From bare land	125	13,135	32,290	2334	138	31,281	79,303
	Total	25,551	273,992	246,260	9005	1172	55,046	611,026

4.4. Detection of Factors Influencing the Spatial Heterogeneity of NDVI

4.4.1. Single Factor Detection

The single factor detection determined the explanatory power (*q* value) of each factor on the spatial heterogeneity of NDVI, ranking them as follows (Table 5): elevation > vegetation type > temperature > precipitation > land use type > soil type > solar radiation > population density > GDP > slope. Elevation is the dominant factor in the spatial heterogeneity of NDVI, with an explanatory power of 64%, which is much larger than that of other factors. Secondly, vegetation type, temperature, precipitation, land use type, and soil type had an explanatory power of not less than 40%, which was the main influence

factor of the NDVI spatial heterogeneity. The explanatory power of solar radiation is 27%, and it is a secondary factor. The explanatory power of other factors is weak, all below 10%, which is basically negligible.

Table 5. The q values of factor detection.

Regions	Ele	Slo	Sol	Pre	Tem	Soi	Veg	Lut	GDP	Pop
SACA	0.637	0.011	0.267	0.492	0.507	0.400	0.518	0.430	0.057	0.072
NYAC	0.480	0.008	0.030	0.425	0.361	0.381	0.288	0.284	0.028	0.106
NYSS	0.128	0.071	0.109	0.115	0.112	0.098	0.075	0.092	0.071	0.041
ETWS	0.568	0.014	0.219	0.351	0.422	0.205	0.438	0.344	0.001	0.001
STAC	0.775	0.021	0.316	0.755	0.687	0.673	0.700	0.540	0.007	0.004

From the point of view of soil and water conservation zones, there are differences in the explanatory power of the factors on the spatial heterogeneity of NDVI. Elevation had the highest explanatory power in all soil and water conservation zones, and its influence was significant in the NYAC, ETWS, and STAC, with the explanatory powers of 48%, 57%, and 78%, respectively, but the explanatory power was significantly lower in the NYSS, at 13%. Vegetation type, temperature, precipitation, land use type, and soil type exhibited explanatory powers exceeding 20% in all regions except for NYSS, where its influence was less pronounced. Solar radiation displayed weak explanatory power, with the values of only 3% and 11% in the NYSS and NYAC, respectively, but relatively higher values of 22% and 32% in the ETWS and STAC, respectively. Slope, GDP, and population density had weak explanatory powers in all the soil and water conservation zones. In the SACA, the explanatory powers of primary and secondary factors for the NDVI spatial heterogeneity were significantly enhanced in the STAC, while other zones experienced varying degrees of weakening, with the most noticeable reduction observed in the NYSS.

4.4.2. Interaction Detection

The interaction detector assessed the explanatory power of interactions between the influencing factors of the NDVI spatial heterogeneity. The results revealed that the q values of interactions between two factors surpassed those of individual factors, demonstrating the relationships of bivariate enhancement and nonlinear enhancement. The explanatory power of the interaction between elevation and other factors is more than 60%. The elevation ∩ vegetation type interaction had the highest explanatory power of 71%, followed closely by elevation ∩ land use type and elevation ∩ solar radiation, both having 70%. Interactions between dominant and primary factors generally exhibited high explanatory powers, with all exceeding 40% (Figure 7a). These interactions demonstrated that the influences of factors on the NDVI spatial heterogeneity were not independent but rather cooperative.

From the perspective of soil and water conservation zones, there are differences in the explanatory power of the interaction between the influencing factors. As shown in Figure 7b–e, in the NYAC, elevation ∩ soil type exhibited the highest explanatory power, followed by elevation ∩ precipitation and soil type ∩ precipitation, all surpassing 56%. In the NYSS, the explanatory power of elevation ∩ solar radiation was the highest, followed by elevation ∩ precipitation and elevation ∩ temperature, both exceeding 25%. In the ETWS, the explanatory power of elevation ∩ temperature is the highest, followed by those of elevation ∩ temperature and elevation ∩ land use type, all surpassing 60%. In the STAC, the top three combinations of factor interactions were elevation ∩ vegetation type, elevation ∩ soil type, and elevation ∩ precipitation, all exceeding 81%. The explanatory powers of the interaction between elevation and other factors were the highest in all soil and water conservation zones, which further verified that the influence of elevation on the spatial heterogeneity of NDVI in the SACA was dominant.

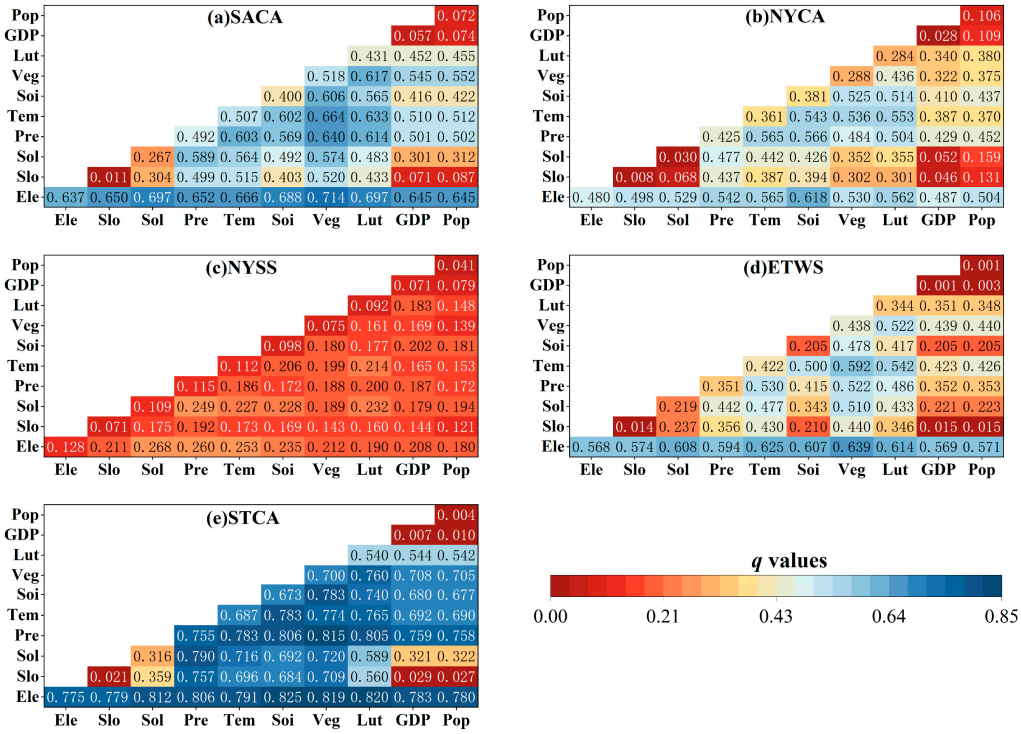

Figure 7. The *q* values of interaction detection.

4.5. Impacts of Climate Change and Human Activities on NDVI Changes

4.5.1. Changes in NDVI under the Influence of Climate Change and Human Activities

$NDVI_{CC}$ and $NDVI_{HA}$ from 2000 to 2019 were subjected to the Theil–Sen trend analysis and the MK significance test, which indicated the characteristics of NDVI changes under the influence of climate change and human activities, respectively. Under the influence of climate change, 86.56% of the study area showed an increasing trend for NDVI, of which 34.23% achieved the required significance level ($p < 0.05$), and these regions were distributed in the Northern STAC, the Western and Northeastern ETWS, and the Northern NYSS. The percentage of the areas with a decreasing NDVI was 13.44%, of which 4.81% achieved the required significance level ($p < 0.05$), mainly at the junction of the STAC and the ETWS (Figure 8a).

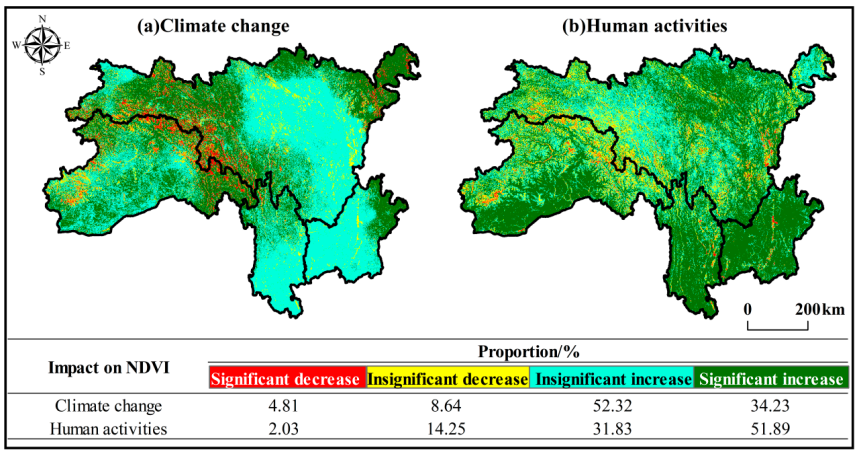

Impact on NDVI	Proportion/%			
	Significant decrease	Insignificant decrease	Insignificant increase	Significant increase
Climate change	4.81	8.64	52.32	34.23
Human activities	2.03	14.25	31.83	51.89

Figure 8. Trends of NDVI under the influence of (**a**) climate change and (**b**) human activities.

Under the influence of human activities, 83.72% of the study area showed an increasing trend for NDVI, of which 51.89% achieved the required significance level ($p < 0.05$), mainly in the NYAC, NYSS, Southern STAC, and Central ETWS. The proportion of areas

with a decreasing NDVI was 16.28%, of which 2.03% achieved the required significance level ($p < 0.05$) and are mainly distributed in the Eastern ETWS and the Northern STAC (Figure 8b).

The impact of climate change was relatively higher in the STAC and the ETWS, with 42.08% and 36.20% of the regions showing a significant level of NDVI trend, compared to 19.44% and 20.29% of the NYAC and the NYSS, respectively. The proportion of the areas with a significant level of NDVI trend in the NYAC and the NYSS under the influence of human activities were 72.43% and 84.52%, respectively, whereas those in the STAC and the ETWS were lower than 50%. The impacts of human activities on the NYAC and the NYSS were relatively higher. Generally speaking, the effects of climate change and human activities on vegetation have both positive and negative effects but mainly focus on improvement, and the positive promotion effect of human activities is stronger than that of climate change.

4.5.2. Driving Mechanism of NDVI Changes

According to Figure 9, which shows the spatial distribution of the NDVI change drivers. The proportion of the areas where NDVI rises were driven by both climate change and human activities was 76.68%, and those areas were mainly distributed in the NYAC, NYSS, Southern STAC, and Northern ETWS. The proportion of the areas where NDVI rises were driven by climate change alone was 3.79%, and these areas were mainly distributed in the Southwest ETWS, and the proportion of the areas where NDVI rises were driven by human activities alone was 5.12%, and these areas were scattered in the North ETWS and the North NYAC. The proportion of the areas where NDVI decreases were driven by both climate change and human activities was 8.42%, and these areas were concentrated at the junction of the ETWS and the STAC. The areas where NDVI decreases were due to climate change alone were scattered in the Western ETWS, with a proportion of 1.93%. The proportion of the areas where NDVI declines were due to human activities alone was 4.07%. These areas were mainly concentrated in the Southern ETWS and the Eastern STAC. Overall, the changes in NDVI are mainly influenced by the combination of climate change and human activities.

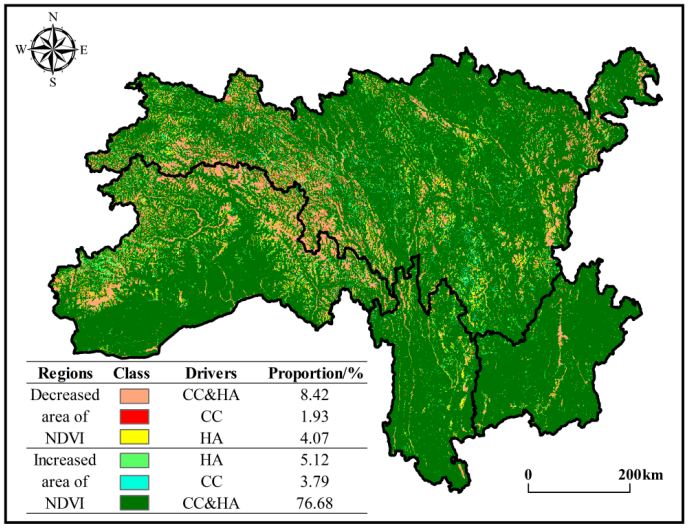

Figure 9. Spatial distribution of NDVI change drivers.

4.5.3. The Relative Contributions of Climate Change and Human Activities to NDVI Changes

The relative contributions of climate change and human activities to NDVI changes were calculated based on θ ($NDVI_{HA}$), θ ($NDVI_{CC}$), and θ (NDVI). Overall, the relative contribution of climate change to NDVI changes was 28.65%, while the relative contributions of human activities was 71.35%. The relative contributions of climate change were higher

in the ETWS and the STAC, with 32.35% and 30.01%, respectively, and the relative contributions of climate change in the NYAC and the NYSS were 21.68% and 19.94%, respectively. The relative contribution of human activities is higher than that of climate change, and the relative contributions of the ETWS, STAC, NYAC, and NYSS were 67.65%, 69.99%, 78.32%, and 80.06%, respectively. To further elaborate on the contribution of climate change and human activities to vegetation growth, the study area was divided into increased and decreased areas based on the slope of NDVI change (Figures 10 and 11).

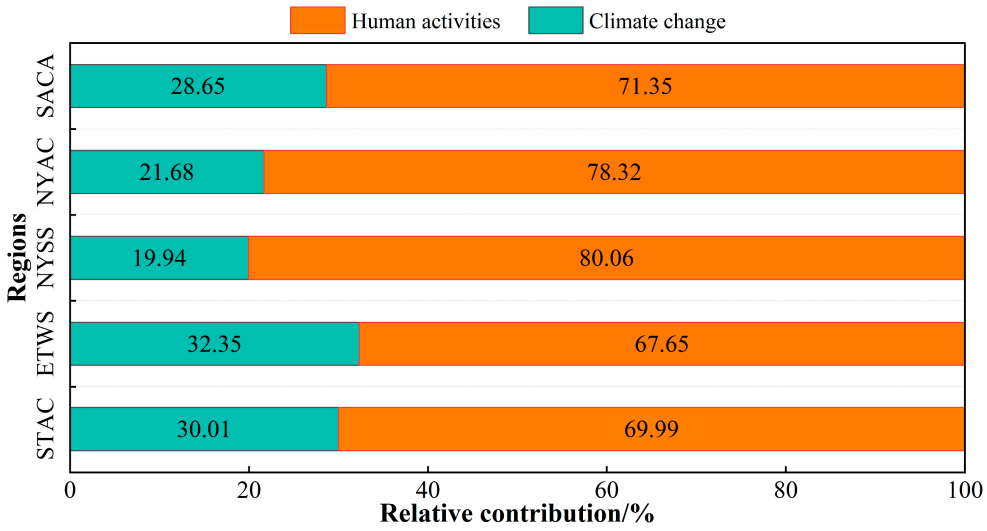

Figure 10. The relative contributions of climate change and human activities in different regions.

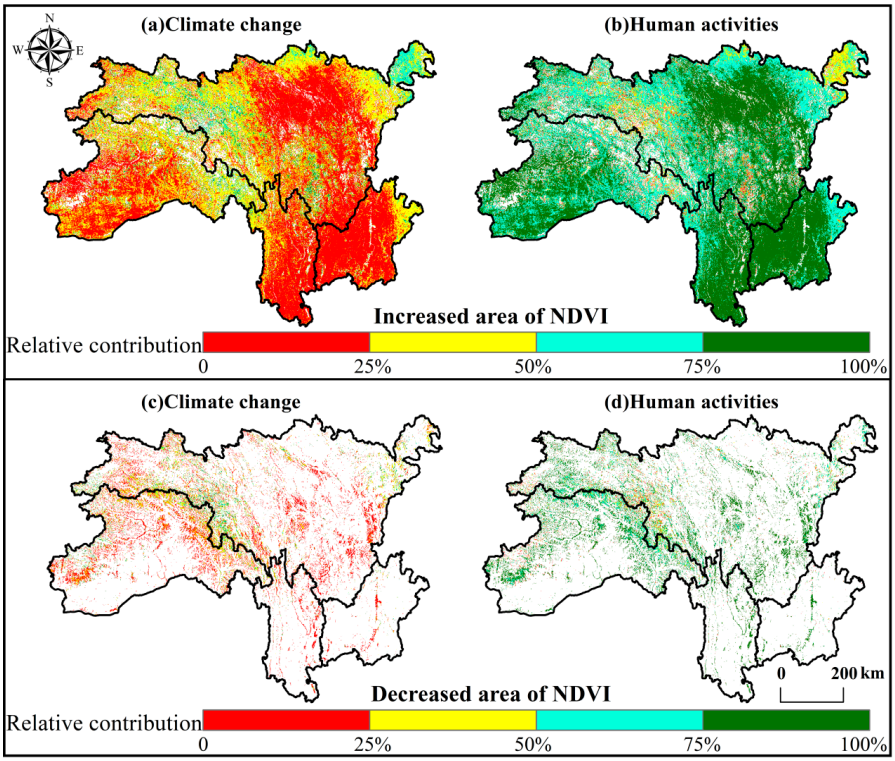

Figure 11. The relative contributions of climate change and human activities to NDVI changes: (**a**) and (**c**) are the relative contribution of climate change in the increased (decreased) area to NDVI, respectively. (**b**,**d**) are the relative contribution of human activities in the increased (decreased) area to NDVI, respectively.

The relative contributions of climate change and human activities within the increased area of NDVI were 28.93% and 71.07%, respectively. The proportion of the areas with an NDVI rise dominated by climate change (relative contribution > 50%) was 16.90%, and these areas were mainly concentrated in the Northeast ETWS and at the junction of the ETWS and the STAC. In the remaining 83.10% of the study area, the relative contribution of human activities exceeded 50% (Figure 11a,b). Within the decreased area of NDVI, the relative contributions of climate change and human activities were 26.96% and 73.04%, respectively. The proportion of the regions with climate change contributing to more than 50% of the NDVI decline was 23.01%, which were mainly distributed at the junction of the ETWS and the STAC. The proportion of the areas where the relative contribution of human activities led to the decrease in NDVI, exceeding 50%, was 76.99%, and these areas were mainly distributed in local regions of the ETWS and the STAC (Figure 11c,d).

5. Discussion

The vegetation cover in the SACA has an obvious spatial heterogeneity, showing a spatial distribution pattern of "high in the southeast and low in the northwest." Elevation is the dominant factor influencing the spatial heterogeneity of vegetation, and its distribution is similar to the distribution of vegetation cover, which is in agreement with the findings of Tao et al. [43]. In the SACA, the terrain is highly undulating and complex, and the change in elevation affects the regional hydrothermal conditions, which in turn affects the spatial distribution of vegetation types and soil types. As the elevation increases, the regional hydrothermal conditions become worse, and the soil is relatively infertile, resulting in poorer vegetation growth [44,45]. In addition, the intensity and extent of human activities are affected by changes in elevation [46]. Therefore, elevation has the highest explanatory power for the spatial differentiation of vegetation in the SACA.

NDVI showed an increasing trend in 85.59% of the study area, and only 14.41% of the area showed a decreasing trend. The relative contribution of climate change to NDVI change was 28.65%. Climate change in the SACA showed warming and drying trends from 2000 to 2019, with temperature and solar radiation increasing at a rate of 0.02 $^{\circ}C \cdot a^{-1}$ and 6.92 $MJ \cdot m^{-2} \cdot a^{-1}$, respectively, and precipitation decreasing at a rate of -3.97 $mm \cdot a^{-1}$. There was a significant variability in the effects of NDVI changes on different climate factors. Overall, temperature and solar radiation were positively correlated with NDVI changes, while precipitation was negatively correlated with NDVI changes. Among them, temperature was the dominant climate factor affecting NDVI changes, which was consistent with the results of Duan et al.'s research [31]. The average annual temperature in the SACA is low, and the increase in temperature is favorable for the decomposition and release of soil nutrients and organic matter. It also can extend the growth season of plants, playing an important role in promoting the growth of vegetation [19]. However, temperature increase has a negative effect on the NDVI trend at the junction between the ETWS and the STAC. Due to an excessive temperature increase in this area, surface evaporation has increased and soil moisture content had decreased, inhibiting vegetation growth [16]. Solar radiation is an important source of photosynthesis for vegetation, and an increase in solar radiation enhances the photosynthetic capacity of vegetation and promotes vegetation growth. Conversely, a decrease in solar radiation inhibits vegetation growth [47]. The trend of precipitation change in the study area increases from the southwest to the northeast. In areas with reduced precipitation, it is negatively correlated with NDVI. The precipitation in the region is relatively low, and an increase in precipitation leads to an increase in soil evaporation and vegetation water consumption, which in turn inhibits vegetation growth. However, this inhibitory effect is insignificant, perhaps because the promoting effects of temperature and solar radiation are stronger than the effect of reduced precipitation. In the Eastern NYSS and the Northern ETWS, the increase in precipitation has a significant promoting effect on vegetation growth. The partial correlation coefficients of temperature and precipitation with NDVI were significantly higher in the area with a higher

precipitation, and there might be a synergistic contribution effect due to the simultaneous increase in temperature and precipitation [48].

The relative contribution of human activities to NDVI change was 71.35%, which was the dominant factor of the NDVI change in the SACA, which is in agreement with the findings of Chen et al. [30]. There is a double effect of the influence of human activities. On the one hand, due to a series of forestry and ecological projects implemented by the state over the years, such as the protection of natural forest resources, the construction of the protection forest system in the Yangtze River Basin, the return of farmland to forest and grassland, and the comprehensive treatment of karst rocky desertification, the bare land has been reduced to a large degree and converted into forest and grassland, which promotes the growth of vegetation, and this is one of the main reasons for the increase in NDVI [43,49]. On the other hand, the degradation of a large amount of forest and grassland due to indiscriminate logging and overgrazing has led to a decrease in NDVI. In addition, with the regional economic development and the accelerated process of urbanization, the expansion of construction land was obvious, and the construction land increased exponentially from 2000 to 2018, encroaching on forest, grassland, and cropland, which inhibited the growth of vegetation [50]. Overall, the positive effects of human activities on vegetation are higher than the negative effects.

6. Conclusions

In this paper, we analyzed the spatiotemporal variation in NDVI in the SACA from 2000 to 2019, as well as the level of influence of driving forces on the NDVI spatial heterogeneity, and we quantified the relative contributions of climate change and human activities to the temporal changes in NDVI. The main conclusions of this paper are as follows: In terms of spatial distribution, NDVI shows a spatial distribution pattern that is high in the southeast and low in the northwest. Elevation was the dominant factor influencing the NDVI spatial heterogeneity, with an explanatory power of 64%, which is much larger than that of other factors. Vegetation type, temperature, precipitation, land use type, and soil type were the main factors affecting the spatial heterogeneity of NDVI. In addition, the explanatory power of the interaction between two factors in all cases was higher than that of the single factor effect, and it showed two kinds of interaction relationships: bivariate enhancement and nonlinear enhancement. In terms of temporal variation, NDVI showed an increasing trend in 85.59% of the study area, and only 14.41% of the area showed a decreasing trend. The main factor affecting NDVI changes was human activities, and climate change was the secondary factor, with relative contributions of 71.35% and 28.65%, respectively. We especially need to pay attention to the junction of the STAC and the ETWS that has a high elevation, a low vegetation cover, and a significant degradation of vegetation due to climate change and human activities from 2000 to 2019, and it should be a key area for ecological restoration in the future.

Author Contributions: Conceptualization, J.L. and T.Z.; methodology, J.L.; formal analysis, J.L., S.Q. and T.Z.; data curation, J.L.; writing—review and editing, J.L., S.Q. and T.Z.; writing—original draft, J.L.; visualization, J.L. and T.Z.; supervision, J.L. and S.Q.; project administration, J.L., S.Q. and T.Z.; funding acquisition, S.Q. All authors have read and agreed to the published version of the manuscript.

Funding: This research was funded by the National Key Research and Development Program of China, grant No. 2022YFF1302903.

Data Availability Statement: The data presented in this study are available upon request from the corresponding author. The data are not publicly available due to the funded projects not yet being completed.

Conflicts of Interest: The authors declare no conflict of interest.

References

1. Slayback, D.A.; Pinzon, J.E.; Los, S.O.; Tucker, C.J. Northern hemisphere photosynthetic trends 1982–1999. *Glob. Chang. Biol.* **2002**, *9*, 1–15. [CrossRef]
2. Loisel, J.; Yu, Z. Surface vegetation patterning controls carbon accumulation in peatlands. *Geophys. Res. Lett.* **2013**, *40*, 5508–5513. [CrossRef]
3. Wang, B.; Jia, K.; Wei, X.; Xia, M.; Yao, Y.; Zhang, X.; Liu, D.; Tao, G. Generating spatiotemporally consistent fractional vegetation cover at different scales using spatiotemporal fusion and multiresolution tree methods. *ISPRS J. Photogramm. Remote Sens.* **2020**, *167*, 214–229. [CrossRef]
4. Morecroft, M.D.; Duffield, S.; Harley, M.; Pearce-Higgins, J.W.; Stevens, N.; Watts, O.; Whitaker, J. Measuring the success of climate change adaptation and mitigation in terrestrial ecosystems. *Science* **2019**, *366*, eaaw9256. [CrossRef]
5. Fensholt, R.; Proud, S.R. Evaluation of Earth Observation based global long term vegetation trends—Comparing GIMMS and MODIS global NDVI time series. *Remote Sens. Environ.* **2012**, *119*, 131–147. [CrossRef]
6. Zhao, Y.; Feng, Q. Identifying the spatiotemporal pattern and driving factors of vegetation dynamics in Shaanxi Province, China. *Geocarto Int.* **2022**, *37*, 17890–17916. [CrossRef]
7. Zhang, S.; Ye, L.; Huang, C.; Wang, M.; Yang, Y.; Wang, T.; Tan, W. Evolution of vegetation dynamics and its response to climate in ecologically fragile regions from 1982 to 2020: A case study of the Three Gorges Reservoir area. *CATENA* **2022**, *219*, 106601. [CrossRef]
8. Huang, J.; Minasny, B.; McBratney, A.B.; Padarian, J.; Triantafilis, J. The location- and scale- specific correlation between temperature and soil carbon sequestration across the globe. *Sci. Total Environ.* **2018**, *615*, 540–548. [CrossRef]
9. Zhong, W.; Chu, T.; Tissot, P.; Wu, Z.; Chen, J.; Zhang, H. Integrated coastal subsidence analysis using InSAR, LiDAR, and land cover data. *Remote Sens. Environ.* **2022**, *282*, 113297. [CrossRef]
10. Li, Y.; Xie, Z.; Qin, Y.; Zheng, Z. Responses of the Yellow River basin vegetation: Climate change. *Int. J. Clim. Chang. Strat. Manag.* **2019**, *11*, 483–498. [CrossRef]
11. Shi, S.; Yu, J.; Wang, F.; Wang, P.; Zhang, Y.; Jin, K. Quantitative contributions of climate change and human activities to vegetation changes over multiple time scales on the Loess Plateau. *Sci. Total Environ.* **2021**, *755*, 142419. [CrossRef] [PubMed]
12. Cleland, E.E.; Chuine, I.; Menzel, A.; Mooney, H.A.; Schwartz, M.D. Shifting plant phenology in response to global change. *Trends Ecol. Evol.* **2007**, *22*, 357–365. [CrossRef] [PubMed]
13. Myers-Smith, I.H.; Kerby, J.T.; Phoenix, G.K.; Bjerke, J.W.; Epstein, H.E.; Assmann, J.J.; John, C.; Andreu-Hayles, L.; Angers-Blondin, S.; Beck, P.S.A.; et al. Complexity revealed in the greening of the Arctic. *Nat. Clim. Chang.* **2019**, *10*, 106–117. [CrossRef]
14. Cui, X.; Xu, G.; He, X.; Luo, D. Influences of Seasonal Soil Moisture and Temperature on Vegetation Phenology in the Qilian Mountains. *Remote Sens.* **2022**, *14*, 3645. [CrossRef]
15. Braswell, B.H.; Schimel, D.S.; Linder, E.; Moore, B., III. The response of global terrestrial ecosystems to interannual temperature variability. *Science* **1997**, *278*, 870–873. [CrossRef]
16. Baumbach, L.; Siegmund, J.F.; Mittermeier, M.; Donner, R.V. Impacts of temperature extremes on European vegetation during the growing season. *Biogeosciences* **2017**, *14*, 4891–4903. [CrossRef]
17. Zhao, J.; Huang, S.; Huang, Q.; Wang, H.; Leng, G.; Fang, W. Time-lagged response of vegetation dynamics to climatic and teleconnection factors. *CATENA* **2020**, *189*, 104474. [CrossRef]
18. Gong, X.; Du, S.; Li, F.; Ding, Y. Study of mesoscale NDVI prediction models in arid and semiarid regions of China under changing environments. *Ecol. Indic.* **2021**, *131*, 108198. [CrossRef]
19. Ma, Y.; Guan, Q.; Sun, Y.; Zhang, J.; Yang, L.; Yang, E.; Li, H.; Du, Q. Three-dimensional dynamic characteristics of vegetation and its response to climatic factors in the Qilian Mountains. *CATENA* **2022**, *208*, 105694. [CrossRef]
20. Jiang, L.; Guli·jiapaer, G.; Bao, A.; Guo, H.; Ndayisaba, F. Vegetation dynamics and responses to climate change and human activities in Central Asia. *Sci. Total Environ.* **2017**, *599–600*, 967–980. [CrossRef]
21. Yan, W.; Wang, H.; Jiang, C.; Jin, S.; Ai, J.; Sun, O.J. Satellite view of vegetation dynamics and drivers over southwestern China. *Ecol. Indic.* **2021**, *130*, 108074. [CrossRef]
22. Foley, J.A.; DeFries, R.; Asner, G.P.; Barford, C.; Bonan, G.; Carpenter, S.R.; Chapin, F.S.; Coe, M.T.; Daily, G.C.; Gibbs, H.K.; et al. Global consequences of land use. *Science* **2005**, *309*, 570–574. [CrossRef] [PubMed]
23. Li, J. Responses of Vegetation NDVI to Climate Change and Land Use in Ordos City, North China. *Appl. Sci.* **2022**, *12*, 7288. [CrossRef]
24. Gemitzi, A.; Banti, M.; Lakshmi, V. Vegetation greening trends in different land use types: Natural variability versus human-induced impacts in Greece. *Environ. Earth Sci.* **2019**, *78*, 172. [CrossRef]
25. Singh, P.; Chaudhuri, A.S.; Verma, P.; Singh, V.K.; Meena, S.R. Earth observation data sets in monitoring of urbanization and urban heat island of Delhi, India. *Geomatics Nat. Hazards Risk* **2022**, *13*, 1762–1779. [CrossRef]
26. Zhao, A.; Zhang, A.; Liu, J.; Feng, L.; Zhao, Y. Assessing the effects of drought and "Grain for Green" Program on vegetation dynamics in China's Loess Plateau from 2000 to 2014. *CATENA* **2019**, *175*, 446–455. [CrossRef]
27. Li, B.; Shi, X.; Lian, L.; Chen, Y.; Chen, Z.; Sun, X. Quantifying the effects of climate variability, direct and indirect land use cover change, and human activities on runoff. *J. Hydrol.* **2019**, *584*, 124684. [CrossRef]

28. Deng, Y.; Wang, M.; Yousefpour, R.; Hanewinkel, M. Abiotic disturbances affect forest short-term vegetation cover and phenology in Southwest China. *Ecol. Indic.* **2021**, *124*, 107393. [CrossRef]
29. Wan, L.; Liu, H.; Gong, H.; Ren, Y. Effects of Climate and Land Use changes on Vegetation Dynamics in the Yangtze River Delta, China Based on Abrupt Change Analysis. *Sustainability* **2020**, *12*, 1955. [CrossRef]
30. Chen, W.; Bai, S.; Zhao, H.; Han, X.; Li, L. Spatiotemporal analysis and potential impact factors of vegetation variation in the karst region of Southwest China. *Environ. Sci. Pollut. Res.* **2021**, *28*, 61258–61273. [CrossRef]
31. Duan, C.; Li, J.; Chen, Y.; Ding, Z.; Ma, M.; Xie, J.; Yao, L.; Tang, X. Spatiotemporal Dynamics of Terrestrial Vegetation and Its Driver Analysis over Southwest China from 1982 to 2015. *Remote Sens.* **2022**, *14*, 2497. [CrossRef]
32. Peng, L.; Deng, W.; Liu, Y. Understanding the Role of Urbanization on Vegetation Dynamics in Mountainous Areas of Southwest China: Mechanism, Spatiotemporal Pattern, and Policy Implications. *ISPRS Int. J. Geo-Inf.* **2021**, *10*, 590. [CrossRef]
33. Hussien, K.; Kebede, A.; Mekuriaw, A.; Beza, S.A.; Erena, S.H. Spatiotemporal trends of NDVI and its response to climate variability in the Abbay River Basin, Ethiopia. *Heliyon* **2023**, *9*, e14113. [CrossRef] [PubMed]
34. Li, S.; Yang, S.; Liu, X.; Liu, Y.; Shi, M. NDVI-Based Analysis on the Influence of Climate Change and Human Activities on Vegetation Restoration in the Shaanxi-Gansu-Ningxia Region, Central China. *Remote Sens.* **2015**, *7*, 11163–11182. [CrossRef]
35. Bao, G.; Qin, Z.; Bao, Y.; Zhou, Y.; Li, W.; Sanjjav, A. NDVI-Based Long-Term Vegetation Dynamics and Its Response to Climatic Change in the Mongolian Plateau. *Remote Sens.* **2014**, *6*, 8337–8358. [CrossRef]
36. Alhumaima, A.S.; Abdullaev, S.M. Tigris Basin Landscapes: Sensitivity of Vegetation Index NDVI to Climate Variability Derived from Observational and Reanalysis Data. *Earth Interact.* **2020**, *24*, 1–18. [CrossRef]
37. Han, W.; Chen, D.; Li, H.; Chang, Z.; Chen, J.; Ye, L.; Liu, S.; Wang, Z. Spatiotemporal Variation of NDVI in Anhui Province from 2001 to 2019 and Its Response to Climatic Factors. *Forests* **2022**, *13*, 1643. [CrossRef]
38. Wang, J.-F.; Zhang, T.-L.; Fu, B.-J. A measure of spatial stratified heterogeneity. *Ecol. Indic.* **2016**, *67*, 250–256. [CrossRef]
39. Han, J.; Zhang, X.; Wang, J.; Zhai, J. Geographic Exploration of the Driving Forces of the NDVI Spatial Differentiation in the Upper Yellow River Basin from 2000 to 2020. *Sustainability* **2023**, *15*, 1922. [CrossRef]
40. Evans, J.; Geerken, R. Discrimination between climate and human-induced dryland degradation. *J. Arid Environ.* **2004**, *57*, 535–554. [CrossRef]
41. Wessels, K.J.; van den Bergh, F.; Scholes, R.J. Limits to detectability of land degradation by trend analysis of vegetation index data. *Remote Sens. Environ.* **2012**, *125*, 10–22. [CrossRef]
42. He, L.; Guo, J.; Jiang, Q.; Zhang, Z.; Yu, S. How did the Chinese Loess Plateau turn green from 2001 to 2020? An explanation using satellite data. *CATENA* **2022**, *214*, 106246. [CrossRef]
43. Tao, J.; Xu, T.; Dong, J.; Yu, X.; Jiang, Y.; Zhang, Y.; Huang, K.; Zhu, J.; Dong, J.; Xu, Y.; et al. Elevation-dependent effects of climate change on vegetation greenness in the high mountains of southwest China during 1982–2013. *Int. J. Clim.* **2018**, *38*, 2029–2038. [CrossRef]
44. Zheng, L.; Xu, J.; Tan, Z.; Xu, L.; Wang, X. Spatial Distribution of Soil Organic Matter Related to Microtopography and NDVI Changes in Poyang Lake, China. *Wetlands* **2019**, *39*, 789–801. [CrossRef]
45. Chen, R.; Yin, G.; Liu, G.; Li, J.; Verger, A. Evaluation and Normalization of Topographic Effects on Vegetation Indices. *Remote Sens.* **2020**, *12*, 2290. [CrossRef]
46. Wang, H.; He, L.; Yin, J.; Yu, Z.; Liu, S.; Yan, D. Effects of Effective Precipitation and Accumulated Temperature on the Terrestrial EVI (Enhanced Vegetation Index) in the Yellow River Basin, China. *Atmosphere* **2022**, *13*, 1555. [CrossRef]
47. Ma, X.; Bai, H.; Deng, C.; Wu, T. Sensitivity of Vegetation on Alpine and Subalpine Timberline in Qinling Mountains to Temperature Change. *Forests* **2019**, *10*, 1105. [CrossRef]
48. Zhang, H.; Chang, J.; Zhang, L.; Wang, Y.; Li, Y.; Wang, X. NDVI dynamic changes and their relationship with meteorological factors and soil moisture. *Environ. Earth Sci.* **2018**, *77*, 582. [CrossRef]
49. Venkatesh, K.; John, R.; Chen, J.; Xiao, J.; Amirkhiz, R.G.; Giannico, V.; Kussainova, M. Optimal ranges of social-environmental drivers and their impacts on vegetation dynamics in Kazakhstan. *Sci. Total Environ.* **2022**, *847*, 157562. [CrossRef]
50. Mekonnen, Z.; Berie, H.T.; Woldeamanuel, T.; Asfaw, Z.; Kassa, H. Land use and land cover changes and the link to land degradation in Arsi Negele district, Central Rift Valley, Ethiopia. *Remote Sens. Appl. Soc. Environ.* **2018**, *12*, 1–9. [CrossRef]